



Spatio-temporal distribution of euphausiids: an important component to understanding ecosystem processes in the Gulf of Alaska and eastern Bering Sea

Kirsten A. Simonsen^{1,2*}, Patrick H. Ressler¹, Christopher N. Rooper¹, and Stephani G. Zador¹

¹National Marine Fisheries Service, Alaska Fisheries Science Centre, Seattle, WA 98115, USA

²National Research Council Research Associateship Programs, Washington, DC 20001, USA

*Corresponding author: e-mail: kirsten.simonsen@noaa.gov

Simonsen, K. A., Ressler, P. H., Rooper, C. N., and Zador, S. G. Spatio-temporal distribution of euphausiids: an important component to understanding ecosystem processes in the Gulf of Alaska and eastern Bering Sea. – ICES Journal of Marine Science, doi: 10.1093/icesjms/fsv272.

Received 31 August 2015; revised 17 December 2015; accepted 23 December 2015.

Euphausiids (principally *Thysanoessa* spp.) are found in high abundance in both the eastern Bering Sea (EBS) and the Gulf of Alaska (GOA). They are an important part of these cold-water coastal and pelagic ecosystems as a key prey item for many species, including marine mammals, seabirds, and fish, forming an ecological link between primary production and higher trophic levels. Acoustic-trawl (AT) survey methods provide a means of monitoring euphausiid abundance and distribution over a large spatial scale. Four years of AT and bottom-trawl survey data (2003, 2005, 2011, and 2013) were available from consistently sampled areas around Kodiak Island, including Shelikof Strait, Barnabas Trough, and Chiniak Trough. We identified euphausiid backscatter using relative frequency response and targeted trawling, and created an annual index of abundance for euphausiids. This index has broad application, including use in the stock assessments for GOA walleye pollock (*Gadus chalcogrammus*) and other species, as an ecosystem indicator, and to inform ecological research. We then used generalized additive models (GAMs) to examine the relationship between relative euphausiid abundance and potential predictors, including pollock abundance, temperature, bottom depth, and primary production. Model results were compared with an updated GAM of euphausiid abundance from the EBS to determine if the factors driving abundance and distribution were consistent between both systems. Temperature was not a strong predictor of euphausiid abundance in the GOA as in the EBS; warmer temperatures and lack of seasonal ice cover in the GOA may be a key difference between these ecosystems. Pollock abundance was significant in both the GOA and the EBS models, but was not a strongly negative predictor of euphausiid abundance in either system, a result not consistent with top-down control of euphausiid abundance.

Keywords: acoustics, Bering Sea, euphausiids, generalized additive models, Gulf of Alaska, pollock.

Introduction

Euphausiids, primarily of the genus *Thysanoessa*, are found in high abundance in both the eastern Bering Sea (EBS) and the Gulf of Alaska (GOA). They are an important part of these cold-water coastal and pelagic ecosystems as a key prey item for many species, including marine mammals, seabirds, and fish, forming an ecological link between primary production and higher trophic levels (Aydin and Mueter, 2007; Aydin *et al.*, 2007; Dorn *et al.*, 2014; Witteveen *et al.*, 2015). Euphausiids, or krill, are particularly important to the diet of walleye pollock (*Gadus chalcogrammus*; hereafter

pollock), which support one of the largest single-species fisheries in the world and the largest in the United States by volume. Catches of pollock in Alaskan waters ranged from 850 000 to 1.36 million t from 2009 to 2013, with an ex-vessel value ranging from \$299.7 to 495.9 million for the same period (Fissel, 2014). Because of the high value of the pollock fishery and the importance of this fish in the EBS and GOA ecosystems, it is important to understand how varying environmental conditions can affect pollock abundance and distribution. One of the key factors may be the distribution of their zooplankton prey, including euphausiids (Hunt *et al.*,

2011, in press; Hollowed *et al.*, 2012; Ressler *et al.*, 2012; Sigler *et al.*, 2012).

In the EBS, previous research including recent shelf-wide acoustic-trawl (AT) surveys (Ressler *et al.*, 2012) has shown that abundance and distribution of euphausiids (primarily *Thysanoessa inermis* and *Thysanoessa raschii*) are correlated with water temperature and the persistence of sea ice in the Bering Sea (Hunt *et al.*, 2011; Hollowed *et al.*, 2012; Ressler *et al.*, 2012, 2014). During cooler years, the abundance of euphausiids is higher than that in warm years with early ice retreat, perhaps due to better feeding conditions associated with spring ice cover, increased ice-associated phytoplankton production, and reduced metabolic demands on euphausiids (Coyle *et al.*, 2011; Hunt *et al.*, 2011, in press; Ressler *et al.*, 2014). Though uncertainty about what controls euphausiid standing stock remains, Ressler *et al.* (2014) and Hunt *et al.* (in press) found that changes in temperatures had a greater effect on euphausiid abundance than did a change in predator (pollock) biomass, implying that euphausiid abundance is influenced more by environmental factors (bottom-up) than by predation.

The GOA euphausiid community contains many of the same euphausiid species as the EBS, but the dominant species are different, and include *T. inermis*, *Thysanoessa spinifera*, and *Euphausia pacifica* with small contributions from other species (Pinchuk *et al.*, 2008). Previous work on zooplankton abundance, including euphausiids, in the GOA focused on the Seward Line (1997–present; Coyle and Pinchuk, 2003; Pinchuk and Hopcroft, 2007; Coyle *et al.*, 2013), and the area around Kodiak Island (Bailey *et al.*, 1995; Wilson, 2009; Wilson *et al.*, 2009, 2013). These studies provided useful information on abundance, species distribution, and size distribution, as well as the timing peaks in biomass and abundance (Coyle and Pinchuk, 2003; Coyle *et al.*, 2013). While these studies focused primarily on copepods, they provide a potentially useful indicator of optimal food conditions for larger zooplankton such as euphausiids, as well as higher trophic levels. Pinchuk and Hopcroft (2007) used this information to examine the growth rates of the three most common species of euphausiids in the GOA, determining that temperature and chlorophyll *a* concentration had the biggest influence on growth. Specifically, temperature-controlled molt rate, while growth increment was affected by food availability, particularly in *T. inermis*, whose growth rate was closely coupled with chlorophyll *a* concentration. Wilson (2009) found that euphausiid abundance west of Kodiak Island was associated with troughs and areas of high flow. Research on euphausiid abundance and distribution in the GOA has been limited in scale, focusing on a relatively small portion of the GOA shelf. Larger-scale studies are often difficult to manage due to cost, time, and personnel constraints. Acoustic surveys offer the means to conduct such large-scale studies of euphausiid distribution, as has been done in the waters surrounding Antarctica (Hewitt and Demer, 2000; Hewitt *et al.*, 2004; Reiss *et al.*, 2008), the east coast of Canada (McQuinn *et al.*, 2013), the Barents Sea (Ressler *et al.*, 2015), and the EBS (De Robertis *et al.*, 2010; Ressler *et al.*, 2012, 2014). Recent GOA-wide acoustic trawl surveys of pollock distribution and abundance conducted in 2003, 2005, 2011, and 2013 offer an opportunity to regularly monitor and better understand factors affecting euphausiid abundance and distribution on a large scale, using survey methods developed in the Bering Sea.

Many similarities exist between the EBS and GOA: they are both high-latitude continental shelf ecosystems inhabited by many of the same species (Aydin *et al.*, 2007). However, there are several differences that have the potential to affect distribution and abundance

of euphausiids: the EBS shelf is wide and flat, and seasonal ice cover plays a major role in structuring the ecosystem, while in the GOA, the shelf is much narrower with prominent bays and troughs, there is no seasonal sea ice, and temperatures are much warmer on average than in the EBS. Furthermore, in the EBS, pollock are the most important predator of euphausiids, where they make up over 60% of all groundfish catches (Aydin *et al.*, 2014). Biomass of pollock in the GOA is roughly 25% of that in the EBS, based on stock assessment reports from both systems (Dorn *et al.*, 2014; Ianelli *et al.*, 2014), while the biomass of other euphausiid predators, such as arrowtooth flounder (*Atheresthes stomias*) and Pacific ocean perch (*Sebastes alutus*), is higher (Aydin *et al.*, 2007). Because of these differences, the roles of temperature and pollock predation as a control mechanism for euphausiid distribution may be much different in the GOA, and there may be other environmental factors that influence distribution.

The relationships between varying environmental conditions, euphausiids, and higher trophic levels are not clear, especially in the GOA. This study sought to expand upon the work of Ressler *et al.* (2012, 2014) to examine the factors influencing the distribution and abundance of euphausiids. The goals of the current study were threefold. First, we wanted to determine if the techniques developed by De Robertis *et al.* (2010) to identify euphausiid backscatter in the EBS were effective in the GOA. Specifically, we wanted to test whether backscatter identified as euphausiids could be effectively ground-truthed using the techniques of De Robertis *et al.* (2010) and Ressler *et al.* (2012), and whether GOA euphausiids had a frequency response similar to that observed in the EBS. Second, we aimed to create an index of abundance for euphausiids in the GOA, based on euphausiid backscatter that can be used to inform the stock assessment for pollock and other species, and to serve as an ecosystem indicator. Finally, we wanted to explore what factors control for euphausiid abundance and distribution in the GOA, and whether the same factors are of similar importance in both systems.

Material and methods

Surveys and data collection

Acoustic backscatter and trawl data were collected during summer AT surveys conducted by NOAA's Alaska Fisheries Science Centre (NOAA-AFSC) aboard the NOAA ships *Oscar Dyson* or *Miller Freeman* using standard acoustic survey techniques (Simmonds and MacLennan, 2005). Honkalehto *et al.* (2010) and Jones *et al.* (2014) provide a detailed description of survey methods. The AT survey data analysed here were collected in the GOA during the summers of 2003, 2005, 2011, and 2013. Acoustic backscatter data were collected with Simrad (reference to trade names does not imply endorsement by the National Marine Fisheries Service, NOAA) EK500 or EK60 echosounders at frequencies including 18, 38, 120, and 200 kHz along parallel transects (Figure 1a); spatial coverage of the survey coverage varied among years. Fish backscatter was sampled with large midwater (Aleutian Wing Trawl; AWT) and bottom (Poly-Northeastern high opening bottom trawl, ca. 7 m vertical opening, PNE) trawls (Stauffer, 2004), while euphausiid backscatter was sampled with a macrozooplankton trawl (Methot trawl; Methot, 1986). Trawl speeds were between 2 and 3 knots ($1-1.5 \text{ m s}^{-1}$).

Catch-per-unit-of-effort data for bottom dwelling fish and invertebrates were also available from the concurrent GOA bottom trawl (BT) surveys conducted by NOAA-AFSC scientists

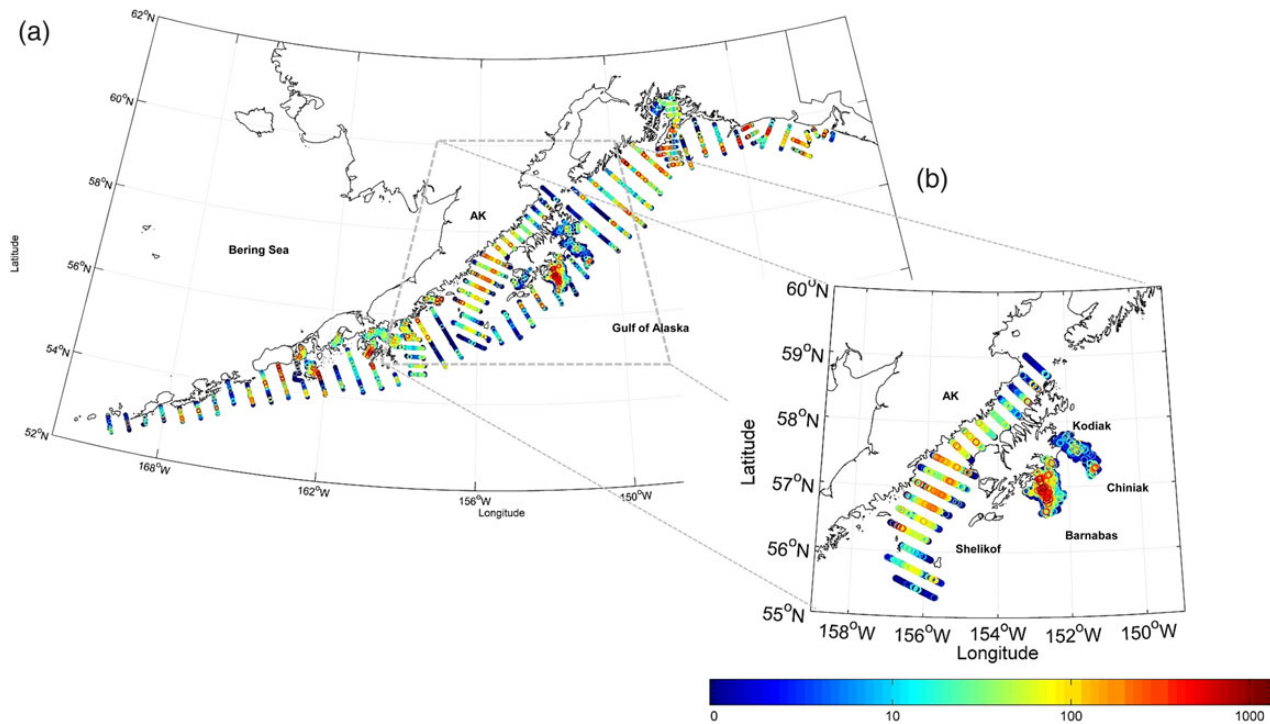


Figure 1. (a) Acoustic backscatter at 120 kHz ($s_A \text{ m}^2 \text{ nautical mile}^{-2}$) identified as euphausiids from the 2013 acoustic trawl survey, as an example of survey coverage and euphausiid distribution. (b) Zoomed in view of euphausiid backscatter in the key, consistently sampled areas including Shelikof Strait, Barnabas Trough, and Chiniak Trough.

aboard chartered fishing vessels in 2003, 2005, 2011, and 2013. The BT survey covers a larger area that encompasses and extends eastward from the AT survey area. It is conducted with a stratified random design, in which the survey area is divided into 59 strata defined by water depth and bottom (von Szalay *et al.*, 2009), targeting depth strata defined by the 100, 200, 300, 400, 500, 600, 700, and 1000 m isobaths. Tows were conducted with a PNE BT towed for ~ 15 min at a speed of 3 knots (1.5 m s^{-1}), resulting in a distance covered of ~ 1.4 km.

Classification of euphausiid backscatter

Euphausiid volume backscatter (S_{euph}) was identified following the techniques of Ressler *et al.* (2012) by comparing the relative frequency response at 18, 38, 120, and 200 kHz (38, 120, and 200 kHz for the 2003 survey) with a trawl-verified reference dataset established by De Robertis *et al.* (2010). To briefly summarize, euphausiid backscatter at 120 kHz was identified using custom routines in both Echoview (Echoview Software, Hobart, Tasmania, Australia) and Matlab (Mathworks, Natick, MA, USA). Volume backscattering strength [S_v , dB re 1 m^{-1} ; see MacLennan *et al.* (2002) for a review of acoustic terminology] was averaged over 5 ping (horizontal) by 5 m (vertical) cells, and then all pairwise differences between S_v at different frequencies were computed for each of these cells. The absolute value of the mean normal deviate (Z -score) over all frequency pairs for each cell was computed relative to the expected pairwise frequency differences for each of several taxonomic groups (including euphausiids, Z_{euph} ; see Table 2 in De Robertis *et al.*, 2010). This mean Z -score indicates how well the observed frequency response matches the expectation for the various taxa and can be used to classify each cell.

Analyses of abundance and distribution are based upon S_{euph} horizontally and vertically integrated at 120 kHz in 926 m (0.5 nautical mile) intervals using an integration threshold of -80 dB to produce s_{Aeuph} ($\text{m}^2 \text{ nautical mile}^{-2}$). We did not attempt to convert s_{Aeuph} to abundance or biomass of euphausiids, as this conversion is highly uncertain in an absolute sense (Hunt *et al.*, in press); no scattering model has been parameterized for euphausiids in the GOA and at present, no measurements of the scattering from a single euphausiid (target strength) are available in this system. Instead, we used s_{Aeuph} as a relative index of vertically integrated euphausiid abundance and biomass.

Ressler *et al.* (2012) identified two possible biases in the classification of euphausiid backscatter data by the method used here. The first is a result of “shadowing” by pollock and other swimbladdered fish, which are significantly stronger scatterers in the water column than euphausiids. The second bias is due to diel vertical migration of euphausiids to the upper water column at night, where they cannot be sampled by vessel-mounted transducers. Corrections were made for both of these biases following Ressler *et al.* (2012). The impact of these corrections on estimated s_{Aeuph} was small, each averaging $< 3\%$.

No 18 kHz backscatter data were available for the 2003 survey because an 18 kHz transducer was not installed on the *Miller Freeman* until 2004 (Honkalehto *et al.*, 2005; Guttormsen and Yasenak, 2007). Because of this, we classified euphausiid backscatter both with and without 18 kHz data in all survey years to evaluate the likely effect on our results of not including that frequency.

Ground-truthing of euphausiid backscatter

The composition of euphausiid backscatter layers was verified using both Methot trawls and with an in-trawl stereo camera system

(CamTrawl) attached to the AWT net (Williams *et al.*, 2010b). Methot tows were targeted on euphausiid layers identified acoustically in summers 2011 and 2013. A total of 13 Methot tows were available, 4 from 2011 and 9 from 2013. Catches were processed following Ressler *et al.* (2012), with larger organisms such as juvenile fish and jellyfish first removed and enumerated, and a subsample of the remaining catch preserved in 5% buffered formalin and sent to the Polish Plankton Sorting and Identification Centre (Szczecin, Poland) for determination of species and length frequency composition. The volume of water filtered by the net was obtained using a calibrated flowmeter and the approximate mouth area. A functional regression (which allows for error in both variables; Ricker, 1973) was fit to the data to assess the null hypothesis of a positive relationship between S_{veuph} and euphausiids captured by the Methot (number m^{-3}) with a slope of 1. Log-transformation of euphausiid abundance improved the normality of regression residuals and model fit, and put both backscatter and net catch on the same scale.

The AWT hauls targeted midwater fish aggregations, but CamTrawl imagery from these hauls was used opportunistically to provide qualitative ground-truthing of euphausiid layers in summer 2013. The CamTrawl produces a series of still stereo images at a rate of four image pairs per second throughout the duration of the trawl (Williams *et al.*, 2010a), which averaged ~ 60 min in length, producing roughly 15 000 frames of still images. Visual analysis began when the doors were set and the trawl was open and fishing, and ended when the net collapsed during haulback. Image frames were then subsampled to every 50th frame, and all euphausiids recorded in the left stereo images were counted. The right image was used for verification of targets when necessary. An average number of euphausiids (counts frame^{-1}) was then calculated and used as a metric for euphausiid abundance in the net haul. The relationship between log-transformed euphausiid counts per frame and log-transformed s_{Aeuph} was determined using functional regression. Unlike the analysis of backscatter from targeted Methot trawls, we used s_{Aeuph} in this regression (instead of the S_{veuph}) because in several of the opportunistic AWT deployments, euphausiid backscatter was below our integration threshold ($S_{\text{veuph}} = -999$ dB, $s_{\text{Aeuph}} = 0$). Since camera placement and lighting was optimized for large fish targets, it was not possible to identify euphausiids to species, to quantitatively estimate euphausiid abundance in numbers m^{-3} , or to measure euphausiid length and orientation from CamTrawl imagery; however, these data did provide a useful qualitative comparison.

Frequency response of GOA euphausiids

We used a subset of the Methot tows used for ground-truthing to empirically estimate the frequency response from GOA euphausiids as in De Robertis *et al.* (2010). Three of the 13 ground-truthing tows from the GOA in 2011–2013 met the restrictive catch composition used by De Robertis *et al.* (2010). Briefly, the average frequency response relative to 38 kHz ($S_{\text{v}18-38}$, $S_{\text{v}120-38}$, and $S_{\text{v}200-38}$) was computed using backscatter measured in the immediate vicinity of Methot trawl paths targeting suspected euphausiid backscatter layers for which the catch contained 100% euphausiids by number after large, rare organisms such as jellyfish were removed. Backscatter likely to be from other taxa was excluded, suspected euphausiid backscatter with signal-to-noise ratio (cf. De Robertis and Higginbottom, 2007; De Robertis *et al.*, 2010) > 10 dB and $S_{\text{v}} > -80$ dB for at least one frequency was averaged into 5 ping by 5 m cells, and then a bootstrapped mean ($n = 50$ cells) of $S_{\text{v}18-38}$, $S_{\text{v}120-38}$, and $S_{\text{v}200-38}$ was computed for each tow. Finally, the

mean and standard deviation was computed for each frequency pair over all tows.

Creating an index of euphausiid abundance for the GOA

An annual index of euphausiid abundance was created from the GOA AT survey data in consistently sampled survey regions (Shelikof Strait, Barnabas Trough, and Chiniak Trough; Figure 1b) as follows:

$$\sum_{n=1}^k A_k \sum_{n=1}^j s_{\text{Aeuph}}, \quad (1)$$

where s_{Aeuph_j} is vertically integrated euphausiid backscatter in the j th interval and A_k is the area of the k th survey region. A one-dimensional geostatistical variance estimate (Petitgas, 1993) was calculated for each region due to the differences in survey transect spacing, and then a variance over all regions was determined by summing variance of the three regions (Rivoirard *et al.*, 2000). This is analogous to the procedure used to compute pollock biomass and estimation error for each region in the AT survey (Honkalehto *et al.*, 2010). The index of euphausiid abundance was created for S_{veuph} classified both with and without 18 kHz data to assess the impact of this frequency on the results.

Modelling of euphausiid abundance in the GOA

Dataset

Data for multiple regression modelling were summarized at the same resolution as the stratified random BT survey stations. Surface and bottom temperature were measured at each BT station with a Seabird SBE-39 bathythermograph placed on the headrope of the PNE BT. The average primary production ($\text{mg C m}^{-2} \text{d}^{-1}$) was estimated from MODIS (Moderate Resolution Imaging Spectroradiometer) ocean colour data and a vertically generalized productivity model (VGPM; Behrenfeld and Falkowski, 1997) available from Oregon State University's Ocean Productivity website (<http://www.science.oregonstate.edu/ocean.productivity>). Following Rooper *et al.* (2014), the data were averaged for May–September of each sampling year, which included the survey sampling period (June–August, for both BT and AT) as well as the peak of the spring and summer phytoplankton blooms, and then interpolated to a $100 \text{ m} \times 100 \text{ m}$ grid covering the GOA shelf before data at each BT survey station were extracted.

A two-dimensional surface of both s_{Aeuph} and vertically integrated pollock biomass density (kg ha^{-1}) was created by kriging the acoustic data from AT survey intervals in each of three study areas (Shelikof, Barnabas, and Chiniak) using the *gstat* (version 1.0-22) and *raster* (version 2.3-40) packages in R (version 3.1.2, R Development Core Team, 2014), with kriging boundaries defined as the extent of each survey area. Values of kriged acoustic data were then extracted at each BT location. We summed the estimates of both acoustic and BT pollock biomass density to create an estimate of total pollock biomass density at each sample location (Ressler *et al.*, 2012; Kotwicki *et al.*, 2015). This estimate may be biased in an absolute sense because: (i) the two surveys sample overlapping portions of the water column near the seabed, and (ii) the acoustic and BT sampling did not take place at exactly the same time (though both BT and AT surveys occur in the same ca. 2-month period). However, we contend that combining pollock biomass density from the two surveys provides a better index of potential predation by pollock upon euphausiids for our purposes than does each survey estimate alone. A comparison of BT and AT

pollock survey estimates found that they were only weakly correlated ($r^2 = 0.022$, $p = 0.0014$, $n = 410$ stations in four surveys), and therefore largely independent of each other for modelling purposes.

Model fitting and evaluation

Generalized additive models (GAMs) were fit to the data using the *mgcv* package (version 1.8-6; Wood, 2006) in R (version 3.1.2, R Development Core Team, 2014). GAM models assume predictors have an additive effect and use smooth functions (penalized regression splines; Wood and Augustin, 2002) to model the effect of the predictors on the response variable. The full model was based upon that developed by Ressler *et al.* (2014) and was used to test whether temperature had a strong predictive effect on euphausiid abundance in the GOA, as was observed in the EBS. The GAM model equation had the following form:

$$\log_{10}(\text{euph} + 10) = s(\log_{10}(pk + 10)) + s(\text{bot_temp}) + s(\text{depth}) + s(PP) + s(\text{avg_sst}) + \text{factor}(\text{region}) + e, \quad (2)$$

where $s(x)$ is the smoothed effect of each covariate, *euph* the s_{Aeuph} (m^2 nautical mile $^{-2}$), *pk* the pollock biomass density (kg ha^{-1}), *bot_temp* the bottom temperature in $^{\circ}\text{C}$, *depth* the bottom depth in m, *PP* the estimated primary production ($\text{mg C m}^2 \text{d}^{-1}$), *avg_sst* the average annual sea surface temperature in $^{\circ}\text{C}$, and *region* the one of the three consistently sampled study regions (Shelikof, Barnabas, or Chiniak; Figure 1b). Knots on smooth terms were limited to $k = 5$ so that the shapes of the partial effects appeared biologically reasonable and to improve interpretability (Peterson *et al.*, 2014). No spatial term was included in this model because there was no evidence of spatial autocorrelation in model residuals. Bottom depth and the region factor served to account for differences in s_{Aeuph} best explained by sampling location. Annual average surface temperature was used as a proxy for year to be consistent with the model used in the EBS (Ressler *et al.*, 2014). Both annual average surface and bottom temperature were important covariates in the model of Ressler *et al.* (2014); summer surface and bottom temperature are only weakly correlated on the stratified middle and outer shelf of the EBS (Stabeno *et al.*, 2001). Similarly, we found that bottom temperature was correlated with surface temperature only in shallowest shelf areas of the GOA, which are well mixed during summer (Stabeno *et al.*, 2004).

Backward variable selection was performed by fitting the full model, and then dropping non-significant terms as determined by: (i) a non-significant *F*-test, (ii) estimated degrees of freedom equal to 1 with 95% confidence intervals (CI) of the partial fit including zero, and (iii) an increase in the Akaike's information criterion (AIC) and the generalized cross-validation (GCV) score for the model (Wood and Augustin, 2002). The model in which all terms were significant was determined to be the best model. Model performance was evaluated using the above statistics and examining model residual plots and partial residuals of covariates to determine whether model assumptions had been met. s_{Aeuph} and pollock biomass density were $\log_{10}(x + 10)$ transformed to approximate normality and to be consistent with the model used by Ressler *et al.* (2014).

GAM models are very flexible and capable of fitting many different types of relationships, and therefore may be subject to overfitting (Ressler *et al.*, 2014). Therefore, to test the robustness of the model predictions and to assess the influence of each year's

data on the shapes of partial effects, we employed leave-one-out cross-validation. This method iteratively leaves one survey year out of the model, fitting the remaining three of the four survey years, and then computing a mean-squared prediction error as a measure of the model's ability to predict the remaining year. The mean-squared prediction error was calculated as follows:

$$\text{mspe}_j = \sum_{n,j} \frac{(\text{predicted euph}_{i,j} - \text{observed euph}_{i,j})^2}{n_j}, \quad (3)$$

where mspe_j is the mean-squared prediction error for survey year j , $\text{predicted euph}_{i,j}$ the s_{Aeuph} predicted by the model for station i during year j , $\text{observed euph}_{i,j}$ the s_{Aeuph} observed at station i during year j , n the number of stations during survey year j , and $\sum_{n,i}$ the sum over all $i = n$ stations in survey j .

Modelling euphausiid abundance in the EBS

Ressler *et al.* (2014) described GAMs of euphausiid abundance in the EBS based on summer AT surveys in 2004 and 2006–2010. The results suggested that temperature was a far better predictor of euphausiid abundance than was predation by pollock, which Ressler *et al.* (2014) interpreted as inconsistent with “top-down” control of euphausiid standing stock by predation. In a review of new research on euphausiid abundance in the EBS, the GAM models of Ressler *et al.* (2014) were updated with an additional year of summer survey observations (Hunt *et al.*, in press). Deviance explained and goodness of fit of the updated model were reduced slightly, but the shapes of the partial effects in the GAM and the interpretation remained similar: water temperature had a strong negative association with euphausiid biomass density, while the effect of pollock in the model was relatively weak.

Here, we update the GAM of EBS euphausiid biomass density for 2004–2012 with the additional of satellite-estimated primary production for the EBS, in parallel with the construction of GAMs for GOA euphausiids in the present manuscript. Primary production estimates for each EBS data location were made using the same procedure used for the GOA (see above), and then a spline function of those data were added to the GAM, creating a model of the form

$$\log_{10}(\text{euph} + 10) \sim s[\log_{10}(pk + 10)] + s(\text{bot_temp}) + s(\text{avg_sst}) + s(PP) + s(\text{lon, lat}), \quad (4)$$

where *euph* indicates euphausiid biomass (kg ha^{-1}), *pk* indicates pollock biomass (kg ha^{-1}) combined from AT and BT surveys, *bot_temp* is the bottom temperature ($^{\circ}\text{C}$) at each location, *avg_sst* the annual average surface temperature ($^{\circ}\text{C}$) in the study area, *PP* the average primary production ($\text{mg C m}^{-2} \text{d}^{-1}$), and *lon, lat* the longitude and latitude of each datum. Logarithmic transformation of *euph* and *pk* was used to improve the structure of model residuals; $s(\text{lon, lat})$ fit the average spatial pattern in the data and minimized spatial-autocorrelation in the residuals. As in the GOA model [Equation (2)], knots on univariate smooth terms were limited to $k = 5$. The bivariate spatial term was not limited in this model. Backward variable selection and leave-one-out cross validation was performed in the same manner as for the GOA models.

Several variations on the best model in each system were explored in order to evaluate: (i) the influence of the addition of the primary production data, (ii) determine whether the conclusions of Ressler *et al.* (2014) and Hunt *et al.* (in press) about the relative importance of temperature in the model still held, and (iii) to compare and

contrast the possible factors controlling euphausiid abundance in the EBS and GOA, Predictive power (deviance explained), model fit (AIC), and plots of partial effects were used to compare the models for each ecosystem.

Results

Ground-truthing of GOA euphausiid backscatter

Overall, euphausiids made up 88% of Methot tow catches in all survey years combined, with a mean length of 18.9 ± 2.16 mm. In 2011, euphausiids made up 93% of Methot tow catches by

number, with *T. inermis* making up 92% of the total. In 2013, euphausiids made up 85% of the catch, with *T. inermis* making up 60% of the catch, *E. pacifica* making up 22% of the catch, and *T. spinifera* making up 13%. Tow coverage in 2013 was more extensive than in 2011, and showed a distinct spatial difference in species composition, with tows to the west composed mainly of *T. inermis*, while tows to the east had an increasing proportion of *T. spinifera* and *E. pacifica* (compare Figure 2a and b).

We expected a positive and proportional (1:1) relationship between S_{veuph} and the number of euphausiids collected in

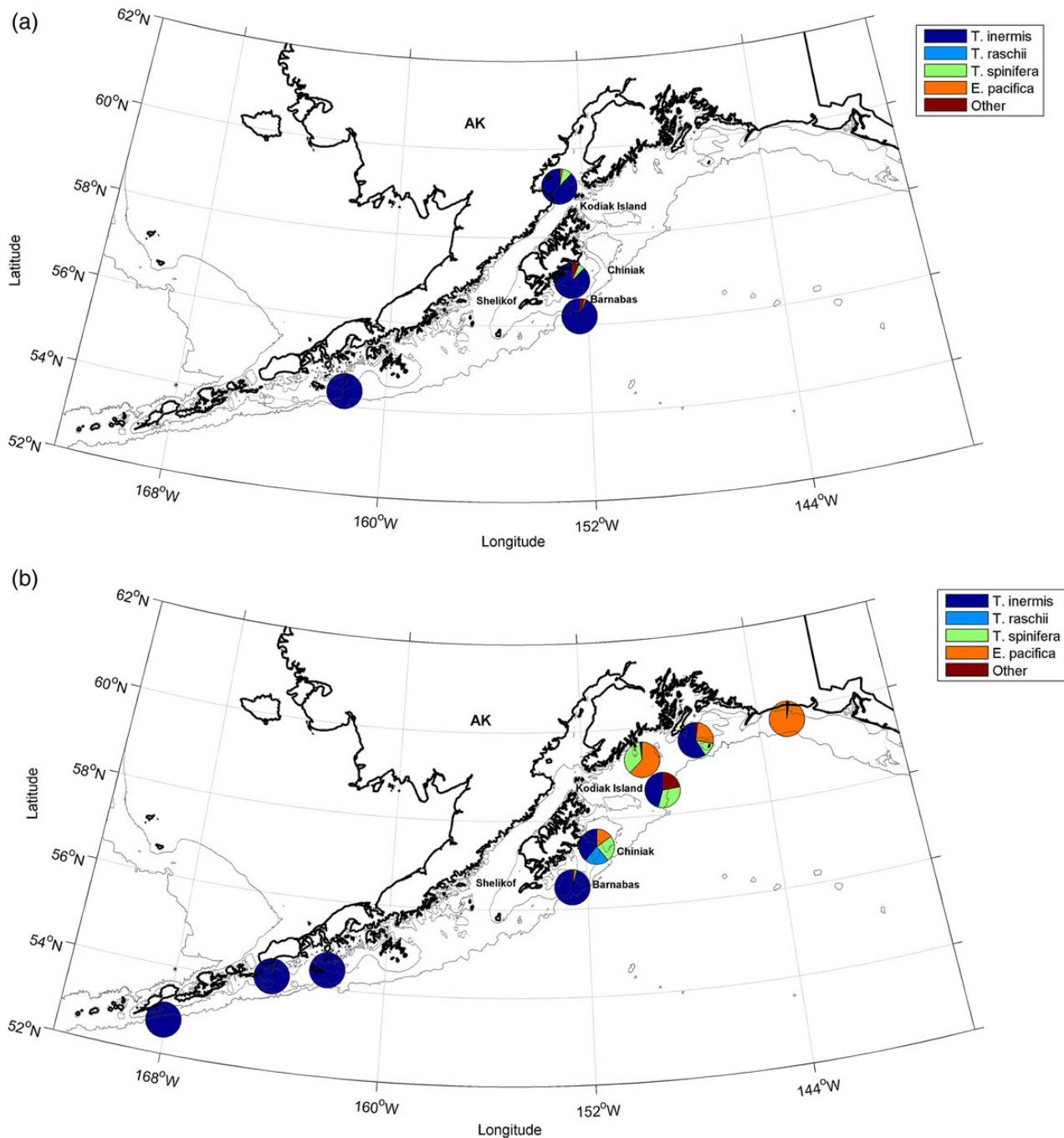


Figure 2. Distribution of euphausiid species identified from Methot tow catch across the GOA in (a) 2011 and (b) 2013. Colours represent different euphausiid species collected. Maroon “other” category includes *T. inspinata*, *T. longipes*, and unidentified euphausiids.

Method net tows. Based on the 13 tows available from 2011 and 2013, we found that euphausiid backscatter (S_V) was positively correlated with Methot catch of euphausiids ($r^2 = 0.20$; Figure 3a), and a 95% CI on the slope of the regression included 1 ($y = 1.310x + 86.360$; Student's t , d.f. = $n - 2$, $\alpha = 0.05$). Variability in this regression was substantial and higher than that in the EBS ($n = 38$; Ressler *et al.*, 2012), likely due in part to the small sample size of tows available.

Analysis of CamTrawl footage resulted in 64 tows for which footage was available for the entire tow, and view was not obstructed during deployment. Euphausiids reliably appeared in CamTrawl images as the AWT reached and passed through euphausiid scattering layers, and CamTrawl counts of euphausiids were positively correlated with s_{Aeuph} (Figure 3b). Three points were left out of the functional regression after being identified as outliers (indicated as triangles in Figure 3b), two of which had residual values > 3 SD from the mean when included in the regression, (open triangles), and one which was determined to be subjected to overlap with a

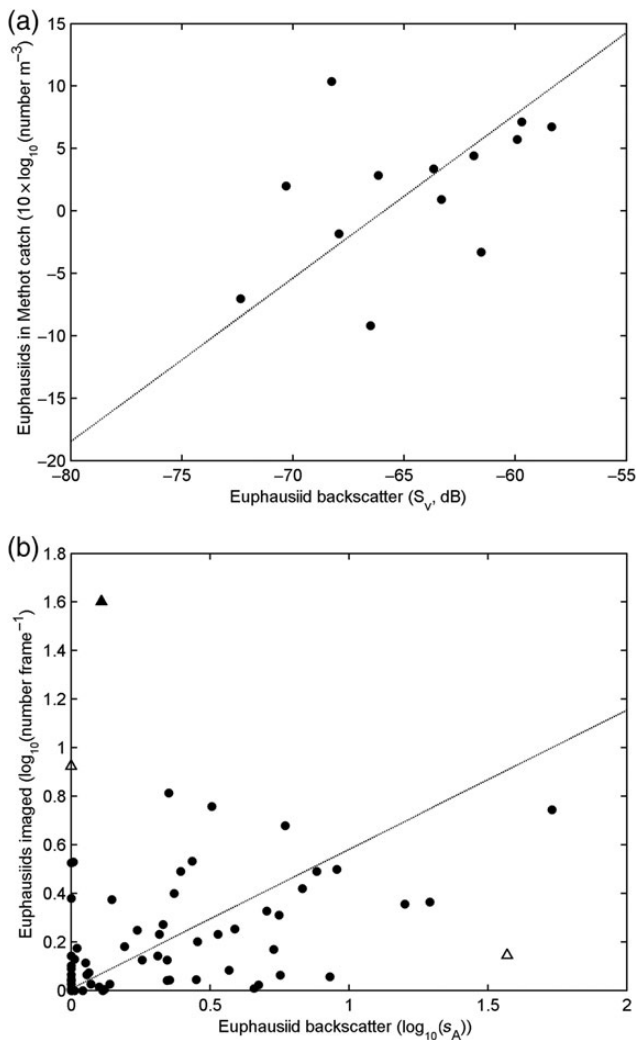


Figure 3. (a) Functional regression of Methot net catch on S_{Veuph} during 2011 and 2013 GOA acoustic trawl surveys ($r^2 = 0.20$, $n = 13$). (b) Functional regression of euphausiids observed in trawl camera imagery on s_{Aeuph} during 2013 GOA acoustic trawl survey ($r^2 = 0.26$, $n = 64$). Three outliers (triangles) were not included in the regression analysis.

dense school of pollock (closed triangle). In the latter case, a high count of euphausiids was identified in CamTrawl footage, while low s_{Aeuph} was observed. The depth layer sampled by this tow had a high density of pollock, which are much stronger scatterers than euphausiids, and therefore dominated the acoustic backscatter in the tow path. No correction for overlap of pollock with euphausiids (see the Material and methods section) could be made to this tow, because backscatter was only analysed in the trawl path, and therefore a “background” s_{Aeuph} could not be calculated. In summary, the relationship between opportunistically imaged euphausiids and s_{Aeuph} was positive ($r^2 = 0.26$, $y = 0.574x + 0.007$, after exclusion of three outliers as indicated) and consistent with our expectation that s_{Aeuph} provides a reliable index of the presence and abundance of euphausiids.

Frequency response of GOA euphausiids

The average frequency response observed for GOA euphausiids in this study was very comparable with that observed by De Robertis *et al.* (2010) for *Thysanoessa* spp. in samples obtained mainly in the EBS (24 of 28 tows were from the EBS), on which our classification method was based, and also to the frequency response reported by Ressler *et al.* (2015) for *Thysanoessa* spp. collected in the Barents Sea (Figure 4). The size range of the animals in all three sources of data was similar, and all datasets included *Thysanoessa* spp., though one of the three tows included a significant fraction of *Euphausia pacifica* (62% of the catch by number) as well. The similarity to observations in other high-latitude ecosystems supports our contention that the euphausiid backscatter classification and survey methods used here are likely to work for the size and species composition of euphausiids present in the GOA.

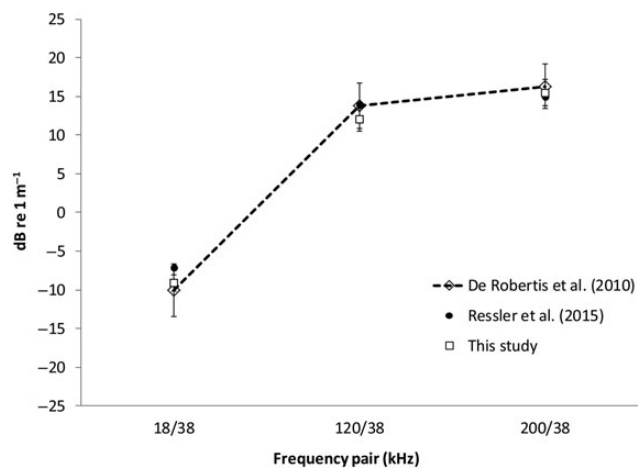


Figure 4. Mean backscatter frequency response relative to 38 kHz for euphausiid aggregations in several high-latitude ecosystems. Error bars indicate + 1 standard deviation from the mean. Net catches from these aggregations contained 100% euphausiids by number. Data from De Robertis *et al.* (2010) were dominated by *Thysanoessa* spp. 15–30 mm in length, obtained in the Bering Sea ($n = 24$ Methot tows) and the GOA ($n = 4$) between 2004 and 2007. Ressler *et al.* (2015) indicate a single tow from the Barents Sea in 2011 containing almost entirely of *Thysanoessa* spp.; lengths were not measured. “This study” indicates data from three tows in the GOA from 2011 to 2013, which contained mainly *T. inermis*, *E. pacifica*, and *T. spinifera* ranging 14–28 mm in length.

Index of euphausiid abundance in the GOA

Euphausiids were found patchily distributed throughout the surveyed area (Figure 1) in all years. Backscatter attributed to euphausiids tended to be higher in the coastal bays and troughs that are characteristic of the GOA when compared with the broad, flat portions of the GOA shelf (Figures 1 and 5a). Of the consistently surveyed areas, Barnabas Trough had the highest mean s_{Aeuph} in all 4 years (Figure 5a). Based on this annual index, GOA euphausiid abundance was highest in 2011 and lowest in 2003 (Figure 5c). There was higher variability around the estimate in 2005 than the other survey years likely due to a more spatially patchy distribution in that year (Figure 6b). If size and acoustical properties of these

euphausiids are assumed to be constant over the 2003–2013 period, these data imply an approximately threefold increase in abundance of euphausiids between 2003 and 2011, suggesting the potential for large interannual variability in abundance of euphausiids in the survey region.

When the 18 kHz data were removed from the classification process, the s_{Aeuph} among survey areas (compare Figure 5a and b) and the annual index changed little (compare Figure 5c and d). However, there was a noticeable increase in the 2005 abundance index (Figure 5d), though CIs for 2005 estimates made with and without the 18 kHz overlapped. Investigation into the cause of this difference suggested it was due in part to the presence of

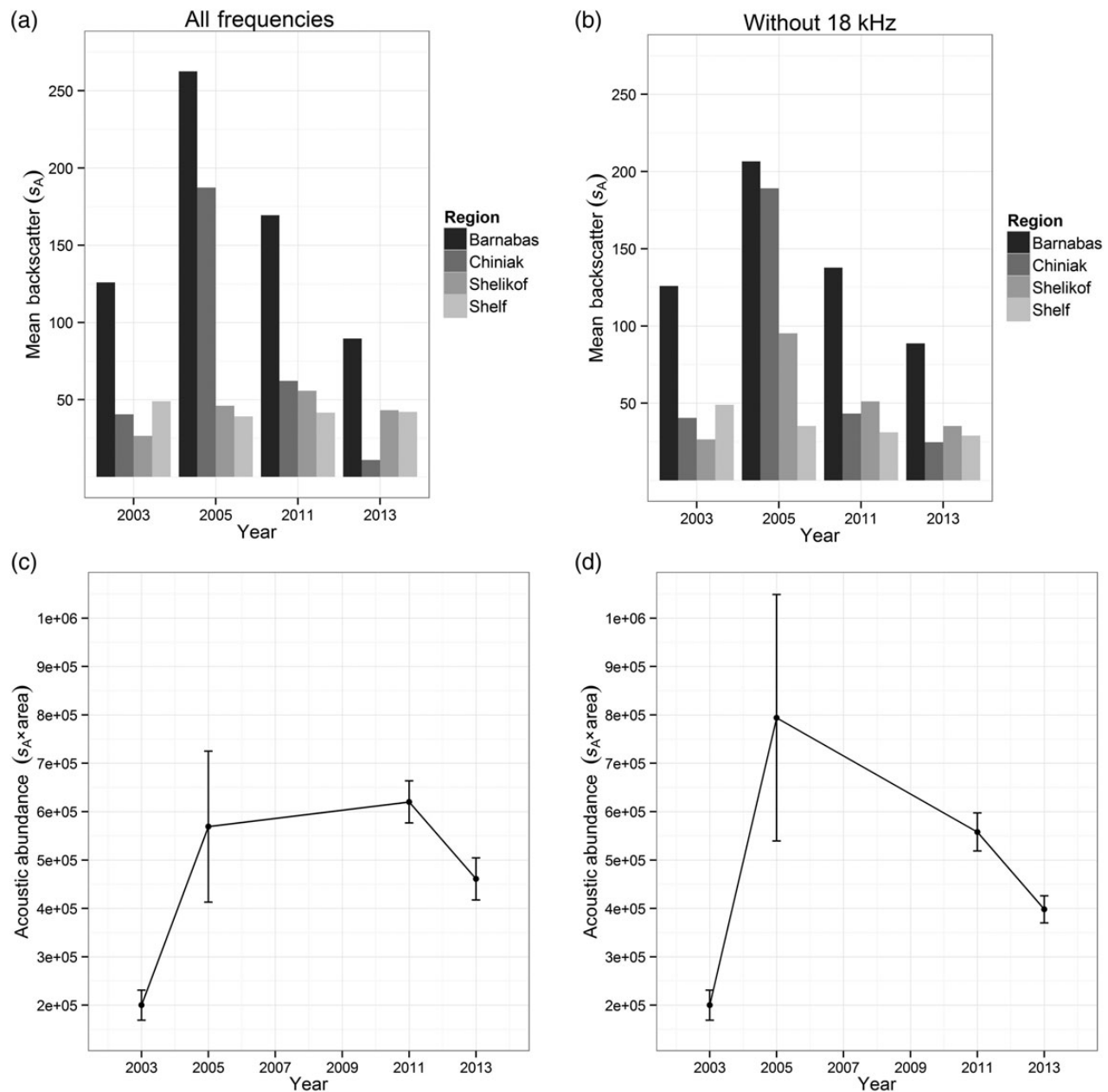


Figure 5. (Top row) Mean euphausiid backscatter density (s_A , m^2 nautical mile $^{-2}$) in the key areas around Kodiak Island, and the surrounding continental shelf, both with all frequencies (a) and with the 18 kHz data removed from analysis (b). (Bottom row) Combined annual index of euphausiid backscatter [Equation (1)] for the key areas around Kodiak Island both with all frequencies (c) and with the 18 kHz data removed from analysis (d). Error bars denote a 95% CI. Note that no 18 kHz data were available in 2003, so the datum for that year is the same in both panels.

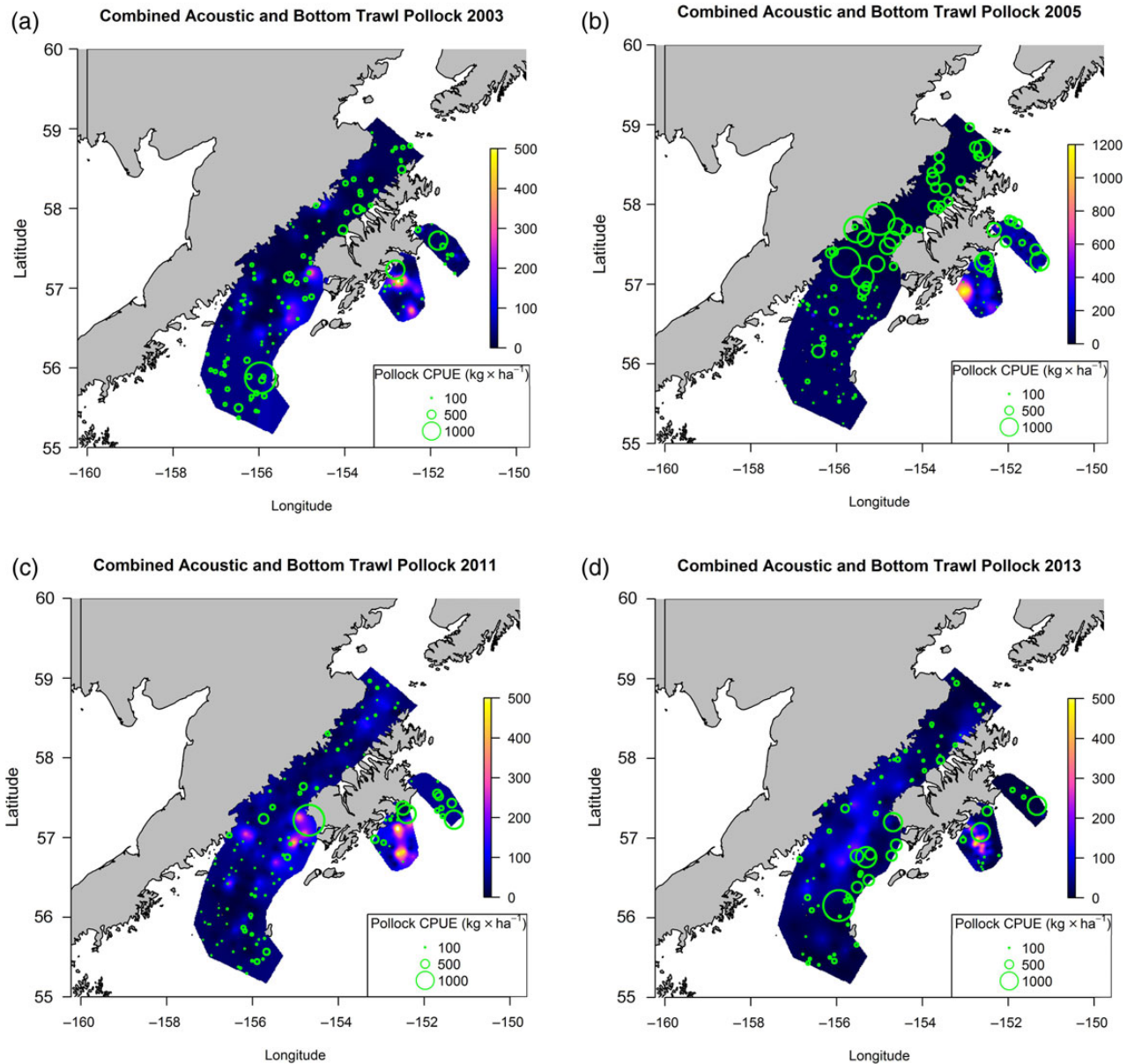


Figure 6. Interpolated euphausiid backscatter from the AT survey (s_{Aeuph} , colour scale), and summed pollock biomass from the AT and BT surveys (kg ha^{-1} ; green circles), in 2003 (a), 2005 (b), 2011 (c), and 2013 (d) for the key areas surrounding Kodiak Island, including Shelikof Strait, Barnabas Trough, and Chiniak Trough. (*Note the different scale for 2005.)

strong volume backscatter at 18 kHz in some areas. This backscatter resembled that of euphausiids at high frequencies but had a higher S_v at 18 kHz than would be expected for euphausiids (De Robertis *et al.*, 2010, Figure 4), and therefore was not identified as S_{veuph} by the multifrequency classification algorithm when 18 kHz data were included. We suspect that this backscatter was a mix of euphausiids and other organisms; however, no net tows were available from these locations to conclusively determine its composition.

We rely on the classification of euphausiids including the 18 kHz data in the remainder of this paper for three reasons. First, the additional frequency generally provides more information for classification, and the techniques originally developed by De Robertis *et al.* (2010) and those used in the EBS analyses (Ressler *et al.*, 2012, 2014) made use of 18 kHz data. Second, although removing the

18 kHz backscatter increased the s_{Aeuph} in 2005 in several areas, it is unlikely that this backscatter was pure euphausiids, as described above. Third, usually this choice does not appear to have a large effect on our results. We suggest that including the 18 kHz data when available, while potentially underestimating the euphausiid backscatter in some areas and some years, produces a more conservative and accurate index of euphausiid abundance.

Model results

Gulf of Alaska

Combined estimates of pollock biomass (kg ha^{-1}) at BT survey stations were plotted over a two-dimensional surface of s_{Aeuph} to visualize the overlap of pollock and euphausiids in space over the four

survey years (Figure 6). Consistent areas of high euphausiid abundance appear within the key areas of the study, including Barnabas Trough and portions of Shelikof Strait to the southwest of Kodiak Island. Conversely, there were no similarly consistent areas of high pollock biomass, and high biomass of pollock did not necessarily overlap with areas of high euphausiid abundance.

Model selection retained model 1.7, a reduced model that included pollock, bottom temperature, primary production, and average annual sea surface temperature, in which all terms were statistically significant, AIC was minimized, and the deviance explained (26.4%) was highest (Table 1, model 1.7). Model residuals were approximately normal and showed no spatial autocorrelation, likely due in part to stratified random design of the BT survey stations. While all model terms were significant, there were no strong relationships between euphausiid abundance and any of the terms (Figure 7). The relationship with pollock (Figure 7a) was relatively flat and similar to that observed in the EBS (Ressler et al., 2014). The relationship with bottom temperature was also relatively flat, with a slightly negative relationship at temperatures $<5^{\circ}\text{C}$ (Figure 7b). The relationship with primary productivity indicated a peak in euphausiid abundance between 1500 and 2000 $\text{g C m}^{-2} \text{d}^{-1}$ with a negative relationship at higher rates of primary productivity (Figure 7c). The relationship with annual-surface temperature was also relatively flat, and was indicative of interannual differences in euphausiid abundance (Figure 7d).

Results from different model scenarios (Table 1) did not suggest that any single term or terms had a disproportionate influence on the model's explanatory power. Leave-one-out cross validation suggested that the results of the full model were robust, as there were no large changes in the shapes of covariate effects (not shown). Deviance explained was lowest when 2003 was left out of the model. Prediction error was rather high relative to the mean s_{Aeuph} in all survey years, and similar among years left out of the model (Table 2).

Results of a GAM model using euphausiid backscatter identified without using the 18 kHz data (not shown) exhibited the same general patterns, with all model terms being significant, but no strong predictors identified, and relationships between s_{Aeuph} and each of the predictor variables were of the same shape.

Eastern Bering Sea

Backward variable selection suggested that the full model (2.1) should be retained: all effects were significant, and the full model had the lowest AIC and highest deviance explained (Table 3). The shape and relative strength of partial effects were quite similar to Ressler et al. (2014) and Hunt et al. (in press): in particular, bottom and surface temperature (Figure 8b and d) had negative effects on predicted euphausiid biomass, while the effect of pollock biomass (Figure 8a) was flat and very modest. The addition of primary production created a small but significant improvement in AIC and deviance explained; the shape of the partial effect (Figure 8e) suggested a positive effect on predicted euphausiid biomass as primary production increases from very low levels, but little effect at larger primary production values. A selection of model scenarios (Table 3) in which single terms were dropped from the full model showed that removal of temperature terms (models 2.4–2.6) produced the largest reductions in explanatory power relative to the full model.

The full model was fairly robust to removal of a single year of survey observations. Model fit and mean-squared prediction error remained fairly consistent (Table 4), all covariates remained

Table 1. GAM of GOA euphausiid biomass density.

Model	Description	Formulation	Deviance explained	AIC	Δ deviance explained
1.1	Full model	$\log(\text{euph} + 10) \sim s[\log(\text{pk} + 10)] + s(\text{bot_temp}) + s(\text{avg_sst}) + s(\text{PP}) + s(\text{bot_depth}) + \text{factor}(\text{region})$	26.4	675.3	0.0
1.2	Drop primary production	$\log(\text{euph} + 10) \sim s[\log(\text{pk} + 10)] + s(\text{bot_temp}) + s(\text{avg_sst}) + s(\text{bot_depth}) + \text{factor}(\text{region})$	21.7	694.6	-4.7
1.3	Drop pollock	$\log(\text{euph} + 10) \sim s(\text{bot_temp}) + s(\text{avg_sst}) + s(\text{PP}) + s(\text{bot_depth}) + \text{factor}(\text{region})$	21.2	691.2	-5.2
1.4	Drop bottom temperature	$\log(\text{euph} + 10) \sim s[\log(\text{pk} + 10)] + s(\text{avg_sst}) + s(\text{PP}) + s(\text{bot_depth}) + \text{factor}(\text{region})$	25.0	677.3	-1.4
1.5	Drop annual average surface temperature	$\log(\text{euph} + 10) \sim s[\log(\text{pk} + 10)] + s(\text{bot_temp}) + s(\text{PP}) + s(\text{bot_depth}) + \text{factor}(\text{region})$	18.4	707.8	-8.0
1.6	Drop all temperature terms	$\log(\text{euph} + 10) \sim s[\log(\text{pk} + 10)] + s(\text{PP}) + s(\text{bot_depth}) + \text{factor}(\text{region})$	18.1	709.9	-8.4
1.7	Drop depth	$\log(\text{euph} + 10) \sim s[\log(\text{pk} + 10)] + s(\text{bot_temp}) + s(\text{avg_sst}) + s(\text{PP}) + \text{factor}(\text{region})$	26.4	673.5	0.0
1.8	Drop bottom temperature and depth	$\log(\text{euph} + 10) \sim s[\log(\text{pk} + 10)] + s(\text{avg_sst}) + s(\text{PP}) + \text{factor}(\text{region})$	24.8	676.3	-1.6

Model 1.1 was the full model used for model selection, while model 1.7 was the best model. Each of the additional variations are shown to demonstrate the reduction in predictive power and model fit when particular terms are dropped. Deviance explained and Akaike information criterion (AIC) and the change in deviance explained are given. Shading indicates large values for deviance explained and small values for AIC. Logarithms are all base 10.

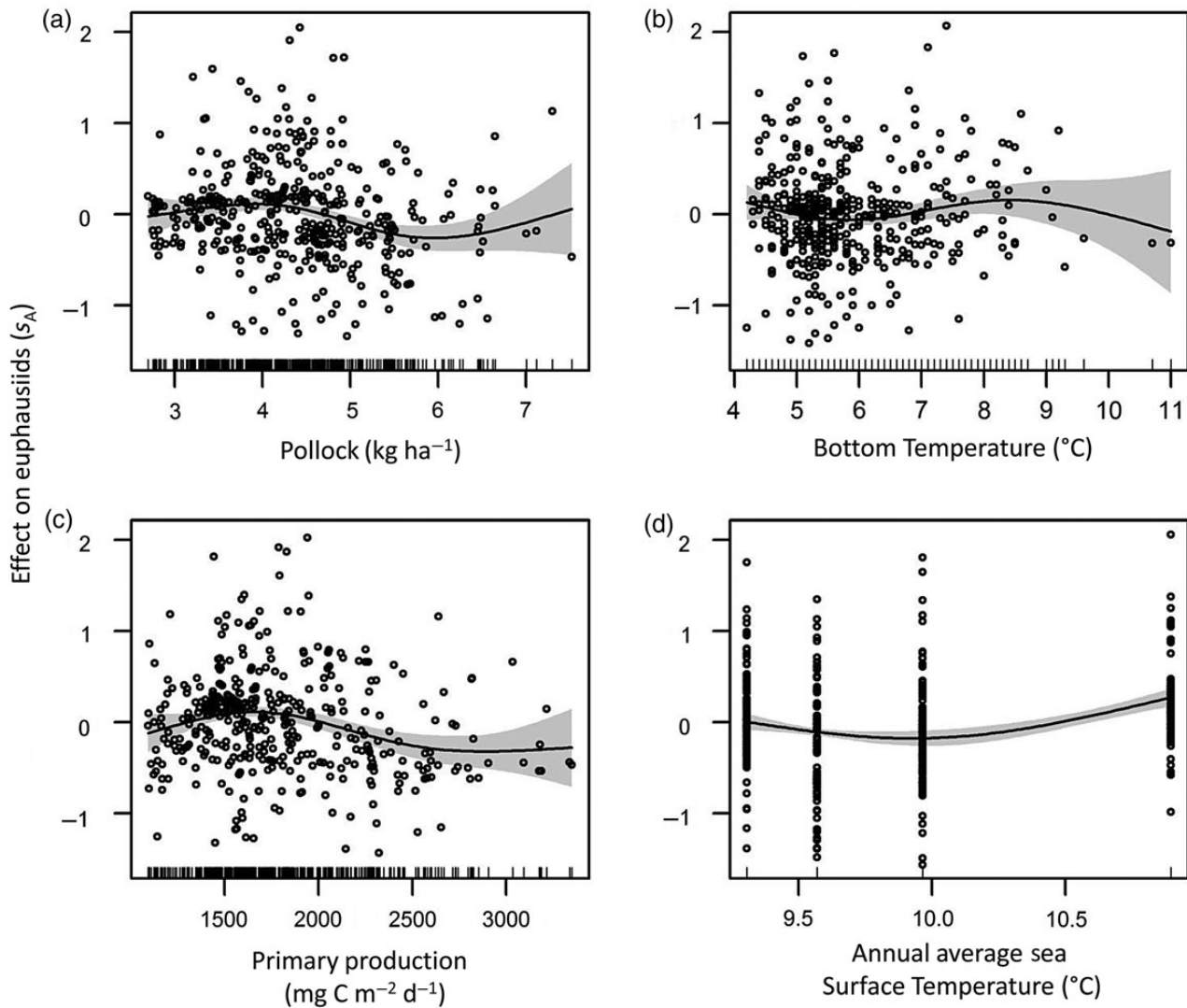


Figure 7. Partial effects plots for smooth functions in the GOA euphausiid GAM model. The units of euphausiid backscatter and pollock biomass have undergone a $\log_{10}(x + 10)$ transformation. Points on the plots are residuals from the full model without the effect of the covariate on the x-axis. Shading denotes a 95% CI around the fit.

Table 2. Leave-one-out cross validation of GAM of GOA euphausiid biomass density.

Year left out	MSPE	Deviance explained	% CV
2013	0.55	36.5	41
2011	0.38	31.6	34
2005	0.36	24.0	34
2003	0.42	23.6	36
Mean	0.43	29.0	36

Each survey year was removed in turn, and then model 1.7 was fit on the remaining data to assess the influence of each year's data on the robustness of the predictive power and the shapes of partial effects in the model. Deviance explained, mean-squared prediction error (MSPE), per cent coefficient of variation (% CV) relative to mean euphausiid density in all survey years are given for each iteration and the mean over all iterations was computed.

statistically significant, and the shapes of partial effects were consistent across all models (not shown). The exception to this was exclusion of summer 2004 observations; as found by [Hunt et al. \(in press\)](#), the results of models fit on the 2004–2012 dataset are sensitive to the

removal of 2004, a very warm year when pollock biomass density was high and euphausiid abundance was low. When 2004 observations were removed (Table 4), model fit decreased and the effect of temperature appeared weaker though still negative; the partial effects of other variables in the model were more or less unchanged.

Comparison of GOA and EBS model results

Annual averages of s_{Aeuph} were somewhat higher in the EBS (mean 95.8, s.d. 35.5) than the GOA (mean 64.5, s.d. 27.6), implying higher euphausiid abundance there. Though the datasets and models of euphausiid abundance are not identical, they are similar enough to directly compare factors affecting euphausiid abundance in the EBS and GOA. The model effect of survey pollock biomass on euphausiid abundance was relatively weak and not strongly negative in the best models from both systems (compare Figures 7a and 8a), an observation not consistent with top-down control by pollock predation. The shape of the effect of primary production on euphausiid biomass was also consistent in

Table 3. GAM of EBS euphausiid biomass density.

Model	Description	Formulation	Deviance explained	AIC	Δ deviance explained
2.1	Hunt et al. (in review) GAM plus primary production	$\log_{10}(\text{euph} + 10) \sim s[\log_{10}(\text{pk} + 10)] + s(\text{bot_temp}) + s(\text{ann_surf_temp}) + s(\text{pp}) + s(\text{lon, lat})$	37.2	2113.4	
2.2	Drop primary production	$\log_{10}(\text{euph} + 10) \sim s[\log_{10}(\text{pk} + 10)] + s(\text{bot_temp}) + s(\text{ann_surf_temp}) + s(\text{lon, lat})$	35.3	2149.9	-1.9
2.3	Drop pollock	$\log_{10}(\text{euph} + 10) \sim s(\text{bot_temp}) + s(\text{ann_surf_temp}) + s(\text{pp}) + s(\text{lon, lat})$	36.6	2124.4	-0.6
2.4	Drop bottom temperature	$\log_{10}(\text{euph} + 10) \sim s[\log_{10}(\text{pk} + 10)] + s(\text{ann_surf_temp}) + s(\text{pp}) + s(\text{lon, lat})$	35.5	2153.1	-1.7
2.5	Drop annual average surface temperature	$\log_{10}(\text{euph} + 10) \sim s[\log_{10}(\text{pk} + 10)] + s(\text{bot_temp}) + s(\text{pp}) + s(\text{lon, lat})$	31.5	2233.3	-5.7
2.6	Drop all temperature terms	$\log_{10}(\text{euph} + 10) \sim s[\log_{10}(\text{pk} + 10)] + s(\text{pp}) + s(\text{lon, lat})$	19.4	2447.5	-17.8

Model 2.1 was the full model used for model selection and all terms were retained as significant. Each of the additional variations are shown to demonstrate the reduction in predictive power and model fit when particular terms are dropped. Deviance explained and Akaike information criterion (AIC) and the change in deviance explained are given. Shading indicates large values for deviance explained and small values for AIC. Logarithms are all base 10.

t- he models, suggesting a positive effect when production increases from very low levels (compare Figures 7c and 8e), but little effect at high levels of primary production. Perhaps the most substantial difference between the models was in the partial effect of temperature: though retained in the best-fitting GAMs for the GOA, neither bottom temperature nor annual average surface temperature had a strong, negative relationship with euphausiid biomass as observed in the EBS (compare Figures 7b and d and 8b and d).

Discussion

Verification of techniques to identify euphausiid backscatter in the GOA

Our results indicate that the euphausiid classification algorithm and survey method developed by De Robertis et al. (2010) and Ressler et al. (2012) are robust enough to work in multiple systems including the GOA, and that s_{Aeuph} is a reliable index of euphausiid biomass and abundance there. Euphausiid size was comparable in the GOA and EBS, and some species were common to both ecosystems. Methot tow catches were successfully used to ground-truth euphausiid backscatter in the GOA. While there was more noise in this regression than was observed in the EBS (Ressler et al., 2012), there was also a much smaller sample size, and only 2 years of data were available for comparison. The relationship between S_{veuph} and euphausiids captured by the Methot trawl was positive and significant with a slope of 1, as hypothesized.

Optical verification and quantification of size, orientation, and abundance of zooplankton targets such as euphausiids remains an active area of research (e.g. cf. review by Benfield et al., 2007; Kubilius et al., 2015). We tested an additional method of verification of euphausiid backscatter using the CamTrawl camera system inside a large midwater trawl. The CamTrawl was designed to observe pollock and other larger fish species captured by the AWT (Williams et al., 2010b), and was not designed to quantify zooplankton. However, euphausiids were regularly visible in CamTrawl images. Though noisy, the regression between s_{Aeuph} and euphausiid counts was positive and significant. Analysis of the imagery was laborious and time-consuming, and would benefit from automation and optimization of the imagery for small zooplankton targets; these remain important challenges in the field. In addition, Ressler et al. (2012) assumed that a bias due to “shadowing” of euphausiid backscatter by collocated pollock was likely, based on the proximity in which euphausiids and pollock were observed in echograms, and a correction was made on a survey-wide basis. CamTrawl imagery in our study visualized and demonstrated this overlap and its effect on measured s_{Aeuph} .

The frequency response of euphausiids identified acoustically in the GOA was very similar to that of euphausiids in the EBS (De Robertis et al., 2010) and the Barents Sea (Ressler et al., 2015). Relative backscatter among frequencies is likely driven principally by euphausiid size, shape, and orientation (e.g. Smith et al., 2013); in these three high-latitude ecosystems, the dominant taxa are *Thysanoessa* spp. and the mean length of individuals is similar. However, target strength is critical for studies that require absolute estimation of euphausiid abundance and biomass (Hunt et al., in press), and depends on material properties of the animals and *in situ* orientation (Smith et al., 2010, 2013). Target strength is difficult to measure and estimate precisely, and it is not clear how consistent it is among ecosystems, species, and time of year. It remains crucial to validate classification and survey methods and measure crucial parameters such as length, species composition, and target strength

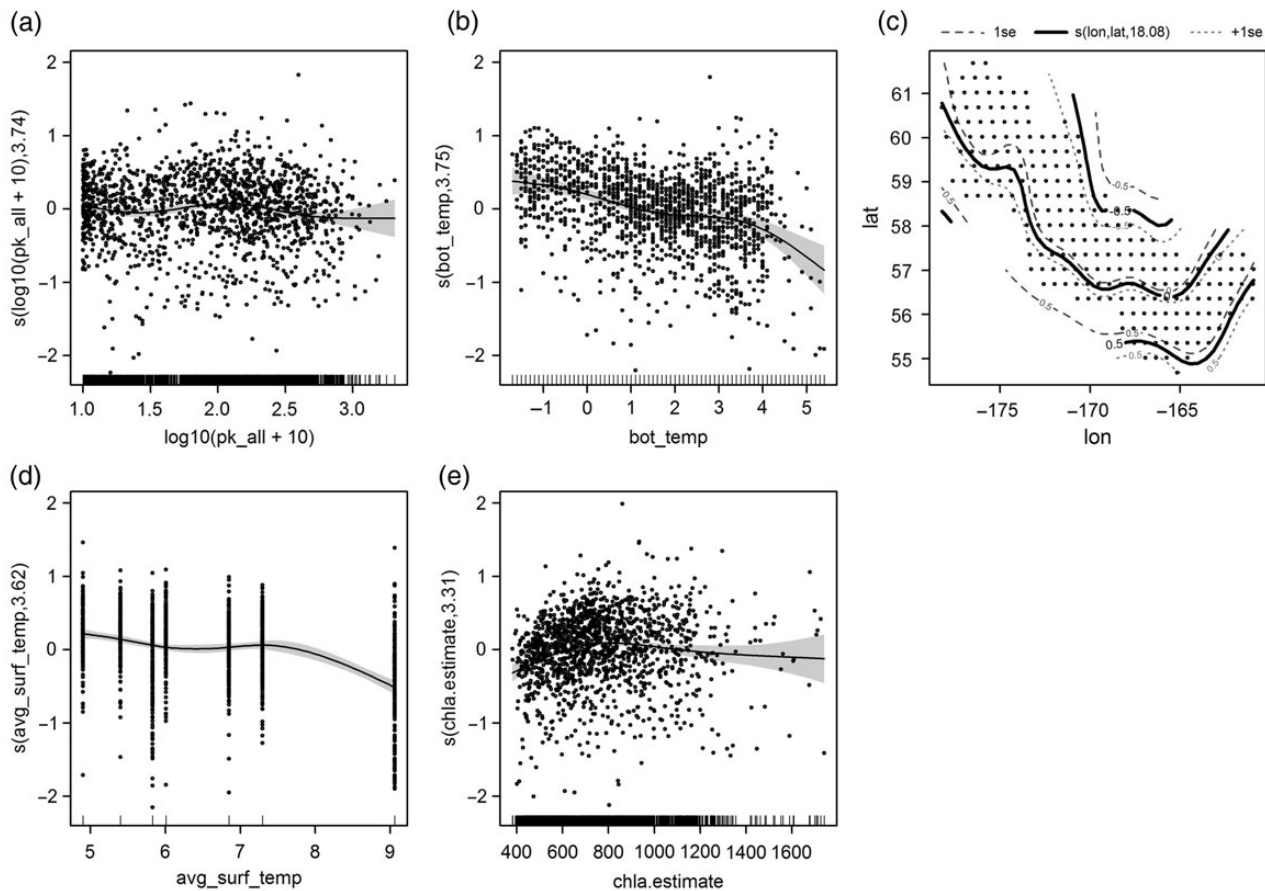


Figure 8. Partial effects plots for smooth functions in the EBS euphausiid GAM model. The units of euphausiid backscatter and pollock biomass have undergone a $\log_{10}(x + 10)$ transformation. Points on the plots are residuals from the full model without the effect of the covariate on the x-axis. Shading denotes a 95% CI around the fit.

Table 4. Leave-one-out cross-validation of GAM of EBS euphausiid biomass density.

Year left out	MSPE	Deviance explained	% CV
2012	0.59	46.6	23
2010	0.28	40.6	16
2009	0.22	37.5	14
2008	0.19	37.9	13
2007	0.20	37.7	14
2006	0.22	39.5	14
2004	1.91	21.8	42
Mean	0.52	37.4	20

Each survey year was removed in turn, and then model 2.1 was fit on the remaining data to assess the influence of each year's data on the robustness of the predictive power and the shapes of partial effects in the full model. Deviance explained, mean-squared prediction error (MSPE), and per cent coefficient of variation (% CV) relative to mean euphausiid density in all survey years are given for each iteration and the mean over all iterations was computed.

in the ecosystems (including the GOA) where survey work and research are accomplished.

Index of euphausiid abundance in the GOA

The annual index of euphausiid abundance created in this study suggested that an increase occurred in the study area between 2003 and

2011, followed by a decrease between 2011 and 2013, although the status in intervening unsampled years is unknown. Caution is required in interpreting such trends in backscatter as changes in abundance or biomass without having euphausiid target strength estimates, but the data we do have suggest consistency in euphausiid length and species composition in the survey area. Thus, relative comparisons between years are likely accurate. [Wilson et al. \(2013\)](#) measured relative euphausiid abundance in 2005, 2007, and 2009 with net sampling around Kodiak Island, which complements the results presented here. The authors found highest abundance of euphausiids in 2005, with a decrease in abundance in 2007 and 2009. As with the current study, [Wilson et al. \(2013\)](#) found that 2005 was the warmest year of their study, and the interannual abundance trends observed were similar.

Because euphausiids are such an important prey item for commercially important fish such as pollock ([Yang and Nelson, 2000](#); [Dorn et al., 2014](#)), it is important to have an understanding of trends in their abundance, as this information can inform both stock assessments and ecosystem assessments. High abundance of euphausiids in the EBS in 2009 is thought to have contributed to the success of the 2008 EBS pollock year class ([Janelli et al., 2014](#)). Such information has not been previously available for the GOA at the scope and scale analysed here, and may be useful for stock assessments of GOA fisheries.

In addition to the potential for direct incorporation into stock assessments, this index has immediate application as an ecosystem indicator. The value of zooplankton indices to studying marine ecosystems has been documented for the North Sea (Beaugrand *et al.*, 2003; Beaugrand, 2005; Buchholz *et al.*, 2010), the Northwest Atlantic (Head and Sameoto, 2007; Kane, 2007), Antarctica (Reid *et al.*, 2005), and Australia (Richardson, 2008). Given the importance of euphausiids as prey for diverse, non-commercially targeted species groups such as forage fish, planktivorous seabirds, and baleen whales (e.g. Yang *et al.*, 2006; Aydin *et al.*, 2007; Witteveen *et al.*, 2015), trends in euphausiid abundance and distribution can have far-reaching impacts on a broad swathe of the marine foodweb. Zooplankton indicators are commonly identified as high priority indicators in neighbouring large marine ecosystems by managers and assessment scientists (Zador, 2014; NOAA CCIEA, 2015). For example, the acoustically determined euphausiid index for the EBS is considered one of the top indicators of ecosystem productivity reflected in an annual report card produced for the North Pacific Fishery Management Council (Zador, 2014), and studies linking euphausiid concentrations and environmental variation are listed as a research need by the Pacific Fisheries Management Council (PFMC, 2013). An advantage of the index derived in this study is the integration of euphausiid trends over a relatively broad scale and variety of habitat features. Thus, a regularly measured euphausiid index will serve as a useful indicator for ecosystem assessments in the GOA with the potential to inform ecological process studies.

Factors driving euphausiid distribution

While all of the factors examined in the GAMs, excluding depth, had statistically significant effects on euphausiid abundance, none were particularly strong predictors of euphausiid abundance and distribution, and the models had modest predictive power. Though euphausiid growth and reproduction in the GOA may be temperature-dependent (Pinchuk and Hopcroft, 2007), there was no strong relationship with water temperature. As to the impact of predation by pollock, we found little support for the hypothesis of strong top-down control in the GOA regression models. The effect of pollock biomass on euphausiids was weak and not strongly negative. Though pollock dominate the midwater fish assemblage of the GOA in biomass terms and euphausiids comprise a large fraction of their diet, their abundance is lower compared with the EBS (Dorn *et al.*, 2014), while several other species, including fish such as capelin (*Mallotus villosus*), Pacific ocean perch, eulachon (*Thaleichthys pacificus*), salmonids, and arrowtooth flounder and marine mammals including humpback whales, are also important predators of euphausiids (e.g. Boldt and Haldorson, 2003; Yang *et al.*, 2006; Aydin *et al.*, 2007; Witteveen *et al.*, 2015). Therefore, it is possible that predation by these species significantly affect the distribution and abundance of euphausiids.

Pinchuk *et al.* (2008) suggested a positive relationship between euphausiid growth and food supply in the GOA, and in our analyses, there was some suggestion of a positive relationship with primary production at low levels of production (Figure 7e). The shape of the relationship with primary productivity was somewhat surprising, as it was positive at low rates and negative at high rates of primary production. This may indicate a threshold level of primary production where euphausiid feeding is saturated, whereby further increases in productivity have little effect. The rates of primary productivity analysed here are based on satellite-derived ocean colour, and therefore only represent the near-surface

layer of primary productivity. It is also possible that average production in summer time is too coarse an index of the timing or quantity of food available to euphausiids.

It may be that physical processes, such as eddies and currents, are an important influence on the distribution of euphausiids in addition to the biological factors examined here. The GOA, particularly the area around Kodiak Island, is a physically dynamic environment, influenced by the Alaska Coastal Current (ACC), which is diverted multiple times as it flows around Kodiak Island, including flowing north on the east side and south on the west side of Barnabas and Chiniak Troughs (Stabeno *et al.*, 2004; Wilson, 2009; Wilson *et al.*, 2013). These patterns, along with temporally stable eddies that form near the shelf break of the GOA yearly, potentially have a large role in aggregating zooplankton such as euphausiids (Pinchuk *et al.*, 2008; Wilson, 2009; Coyle *et al.*, 2013). While there is some evidence that eddies existed near the survey area during the years of this study (Ladd, 2007; Ladd *et al.*, 2007, 2015), the role of advection by large-scale currents as well as meso-scale eddies on euphausiid distribution was beyond the scope of our study but is an active area of research (Coyle and Pinchuk, 2005; Pinchuk *et al.*, 2008; Coyle *et al.*, 2013; Ladd *et al.*, 2015).

Comparison with EBS

Despite the addition of average estimated primary production as an additional covariate, the results of GAMs for EBS euphausiids were more or less consistent with Ressler *et al.* (2014) and Hunt *et al.* (in press): there is a strong negative relationship between water temperature and euphausiid biomass density, but little evidence for a strong effect of predation by pollock, the single largest predator on euphausiids in the EBS. Primary production added a modest amount of prediction power (Table 4), and the shape of the partial effect (positive at low levels of production, rather flat at higher levels) was somewhat intuitive, if increased primary production corresponds to increases in euphausiid food production and availability (Figure 8e). However, the May–September averages of satellite-based primary production estimates would not include ice-associated primary production in early spring.

Pollock biomass was not a strong predictor of euphausiid abundance in either the GOA or the EBS, which is inconsistent with the hypothesis of top-down control by pollock predation as the primary force driving euphausiid abundance. The apparent relationship between euphausiids and water temperature differed; however, it was strongly negative for both bottom temperature and annual average surface temperature in the EBS (Figure 8b and d), but not so in the GOA, where the temperature relationships were rather flat or slightly positive (Figure 7, panels b and d). Crucial differences may be that the EBS is seasonally ice-covered and has much colder temperatures: for bottom temperature, below zero temperatures are common and maximum temperatures were rarely above 5°C even in summer (Figure 8b). The mechanism for the negative effect of temperature on euphausiid biomass in the EBS is not known, but there has been a great deal of speculation about it. The prevailing hypotheses are that: (i) spring ice-associated primary production provides a pivotal source of food for feeding and reproducing euphausiids and/or (ii) metabolic demands are sufficiently reduced by cold water temperatures that survival at a population level increases (Coyle *et al.*, 2011; Hunt *et al.*, 2011; Ressler *et al.*, 2014; Sigler *et al.*, accepted for publication; Hunt *et al.*, in press). The lack of a strong relationship with bottom temperature in the GOA may be due to the lack of seasonal ice cover, warmer and less variable summertime temperatures in this

system, or variable effects of localized habitat complexity including eddies and currents. These apparent differences in temperature-related, bottom-up forcing have implications for ecosystem conditions under future climate scenarios (e.g. Hollowed *et al.*, 2011; Ianelli *et al.*, 2011; Mueter *et al.*, 2011; McBride *et al.*, 2014; Sigler *et al.*, accepted for publication), if the GAM results we present are indicative of euphausiid population response to temperatures in future years. When the north Pacific warms as expected over the next century, it may mean reduced euphausiid abundance in the EBS, but little difference in the GOA.

Acknowledgements

This study, including a National Research Council (NRC) post-doctoral appointment for K. Simonsen, was supported by the North Pacific Research Board (Project 1208, publication number 577) and the NOAA Alaska Fisheries Science Centre (NOAA-AFSC). It was improved by the comments of S. Barbeaux, A. De Robertis, and M. Dorn. The recommendations and general content presented in this paper do not necessarily represent the views or official position of the US Department of Commerce, the National Oceanic and Atmospheric Administration, or the National Marine Fisheries Service.

References

- Aydin, K., Barbeaux, S. J., Barnard, D., Chilton, L., Clark, B., Conners, M. E., Conrath, C., *et al.* 2014. Stock assessment and fishery evaluation report for the groundfish resources of the Bering Sea/Aleutian Islands regions for 2014. North Pacific Fishery Management Council, Anchorage, AK. <http://www.afsc.noaa.gov/REFM/docs/2013/EBSpollock.pdf>.
- Aydin, K., Gaichas, S., Ortiz, I., Kinzey, D., and Friday, N. 2007. A comparison of the Bering Sea, Gulf of Alaska, and Aleutian Islands large marine ecosystems through food web modeling. US Department of Commerce, NOAA Technical Memorandum, NMFS-AFSC-178. 298 pp. <http://www.afsc.noaa.gov/Publications/AFSC-TM/NOAA-TM-AFSC-178.pdf>.
- Aydin, K., and Mueter, F. 2007. The Bering Sea—a dynamic food web perspective. *Deep Sea Research II*, 54: 2501–2525.
- Bailey, K. M., Canino, M. F., Napp, J. M., Spring, S. M., and Brown, A. L. 1995. Contrasting years of prey levels, feeding conditions and mortality of larval walleye pollock *Theragra chalcogramma* in the western Gulf of Alaska. *Marine Ecology Progress Series*, 119: 11–23.
- Beaugrand, G. 2005. Monitoring pelagic ecosystems using plankton indicators. *ICES Journal of Marine Science*, 62: 333–338.
- Beaugrand, G., Brander, K. M., Lindley, J. A., Souissi, S., and Reid, P. C. 2003. Plankton effect on cod recruitment in the North Sea. *Nature*, 426: 661–664.
- Behrenfeld, M. J., and Falkowski, P. G. 1997. Photosynthetic rates derived from satellite-based chlorophyll concentration. *Limnology and Oceanography*, 42: 1–20.
- Benfield, M. C., Grosjean, P., Culverhouse, P. F., Irigoien, X., Sieracki, M. E., Lopez-Urrutia, A., Dam, H. G., *et al.* 2007. RAPID: research on automated plankton identification. *Oceanography*, 20: 172–187. <http://dx.doi.org/10.5670/oceanog.2007.63>.
- Boldt, J. L., and Haldorson, L. J. 2003. Seasonal and geographic variation in juvenile pink salmon diets in the northern Gulf of Alaska and Prince William Sound. *Transactions of the American Fisheries Society*, 132: 1035–1052.
- Buchholz, F., Buchholz, C., and Weslawski, J. M. 2010. Ten years after: krill as indicator of change in the macro-zooplankton communities of two Arctic fjords. *Polar Biology*, 33: 101–113.
- Coyle, K. O., Eisner, L. B., Mueter, F. J., Pinchuk, A. I., Janout, M. A., Cieciel, K. D., Farley, E. V., *et al.* 2011. Climate change in the southeastern Bering Sea: impacts on pollock stocks and implications for the oscillating control hypothesis. *Fisheries Oceanography*, 20: 139–156.
- Coyle, K. O., Gibson, G. A., Hedstrom, K., Hermann, A. J., and Hopcroft, R. R. 2013. Zooplankton biomass, advection and production on the northern Gulf of Alaska shelf from simulations and field observations. *Journal of Marine Systems*, 128: 185–207.
- Coyle, K. O., and Pinchuk, A. I. 2003. Annual cycle of zooplankton abundance, biomass and production on the northern Gulf of Alaska shelf, October 1997 through October 2000. *Fisheries Oceanography*, 12: 327–338.
- Coyle, K. O., and Pinchuk, A. I. 2005. Seasonal cross-shelf distribution of major zooplankton taxa on the northern Gulf of Alaska shelf relative to water mass properties, species depth preferences and vertical migration behavior. *Deep Sea Research II: Topical Studies in Oceanography*, 52: 217–245.
- De Robertis, A., and Higginbottom, I. 2007. A post-processing technique to estimate the signal-to-noise ratio and remove echosounder background noise. *ICES Journal of Marine Science*, 64: 1282–1291.
- De Robertis, A., McKelvey, D. R., and Ressler, P. H. 2010. Development and application of empirical multifrequency methods for backscatter classification in the North Pacific. *Canadian Journal of Fisheries and Aquatic Sciences*, 67: 1459–1474.
- Dorn, M., Aydin, K., Jones, D., Palsson, W., and Spalinger, K. 2014. Assessment of the Walleye Pollock Stock in the Gulf of Alaska. *In* Stock Assessment and Fishery Evaluation Report for the Groundfish Resources of the Gulf of Alaska for 2014, pp. 53–170. North Pacific Fishery Management Council, Anchorage, AK. <http://www.afsc.noaa.gov/REFM/Docs/2014/GOApollock.pdf>.
- Fissel, B. E. 2014. Economic indices for the North Pacific groundfish fisheries: calculation and visualization. US Department of Commerce, NOAA Technical Memorandum, NMFS-AFSC-279. 47 pp.
- Guttormsen, M. A., and Yasenak, P. T. 2007. Results of the 2003 and 2005 echo integration-trawl surveys in the Gulf of Alaska during summer, Cruises MF2003-09 and OD2005-01. AFSC Processed Rep. 2007-04, 61 pp. Alaska Fisheries Science Center, National Marine Fisheries Service, NOAA, Seattle, WA.
- Head, E. J. H., and Sameoto, D. D. 2007. Inter-decadal variability in zooplankton and phytoplankton abundance on the Newfoundland and Scotian shelves. *Deep Sea Research II*, 54: 2686–2701.
- Hewitt, R. P., and Demer, D. A. 2000. The use of acoustic sampling to estimate the dispersion and abundance of euphausiids, with an emphasis on Antarctic krill, *Euphausia superba*. *Fisheries Research*, 47: 215–229.
- Hewitt, R. P., Watkins, J., Naganobu, M., Sushin, V., Brierley, A. S., Demer, D., and Kasatkina, S., *et al.* 2004. Biomass of Antarctic krill in the Scotia Sea in January/February 2000 and its use in revising an estimate of precautionary yield. *Deep Sea Research II*, 51: 1215–1236.
- Hollowed, A. B., Barange, M., Ito, S.-I., Kim, S., Loeng, H., and Peck, M. 2011. Effects of climate change on fish and fisheries: forecasting impacts, assessing ecosystem responses, and evaluating management strategies. *ICES Journal of Marine Science*, 68: 984–985.
- Hollowed, A. B., Barbeaux, S., Farley, E., Cokelet, E. D., Kotwicki, S., Ressler, P. H., Spital, C., *et al.* 2012. Effects of climate variations on pelagic ocean habitats and their role in structuring forage fish distributions in the Bering Sea. *Deep Sea Research II*, 65–70: 230–250.
- Honkalehto, T., McCarthy, A., Ressler, P., Stienessen, S., and Jones, D. 2010. Results of the acoustic-trawl survey of walleye pollock (*Theragra chalcogramma*) on the U.S. and Russian Bering Sea shelf in June–August 2009 (DY0909). AFSC Processed Rep. 2010-03, 57 pp. Alaska Fisheries Science Center, NOAA, National Marine Fisheries Service, Seattle, WA.
- Honkalehto, T., McKelvey, D., and Williamson, N. 2005. Results of the March 2005 echo integration-trawl survey of walleye pollock (*Theragra chalcogramma*) in the southeastern Aleutian Basin near Bogoslof Island, Cruise MF2005-03. AFSC Processed Report 2005-05, 37 pp. Alaska Fisheries Science Center, National Marine Fisheries Service, NOAA, Seattle, WA.

- Hunt, G. L., Jr., Coyle, K. O., Eisner, L., Farley, E. V., Heintz, R., Mueter, F., Napp, J. M., *et al.* 2011. Climate impacts on eastern Bering Sea food webs: a synthesis of new data and an assessment of the Oscillating Control Hypothesis. *ICES Journal of Marine Science*, 68: 1230–1243.
- Hunt, G. L., Jr., Ressler, P. H., Gibson, G. A., De Robertis, A., Aydin, K., Sigler, M. F., Ortiz, I., *et al.* in press. Euphausiids in the Eastern Bering Sea: a synthesis of recent studies of euphausiid production, consumption and population control.
- Ianelli, J. N., Hollowed, A. B., Haynie, A. C., Mueter, F. J., and Bond, N. A. 2011. Evaluating management strategies for eastern Bering Sea walleye pollock (*Theragra chalcogramma*) in a changing environment. *ICES Journal of Marine Science*, 68: 1297–1304.
- Ianelli, J. N., Honkalehto, T., Barbeaux, S., and Kotwicki, S. 2014. Assessment of the walleye pollock stock in the Eastern Bering Sea. In Stock Assessment and Fishery Evaluation Report for the Groundfish Resources of the Bering Sea/Aleutian Islands regions for 2014, pp. 51–156. North Pacific Fishery Management Council, Anchorage, AK. <http://www.afsc.noaa.gov/REFM/docs/2014/EBSpollock.pdf>.
- Jones, D. T., Ressler, P. H., Stienessen, S. C., McCarthy, A. L., and Simonsen, K. A. 2014. Results of the acoustic-trawl survey of walleye pollock (*Gadus chalcogrammus*) in the Gulf of Alaska, June–August 2013 (DY2013-07). AFSC Processed Report 2014-06, 95 pp. Alaska Fisheries Science Center, NOAA, National Marine Fisheries Service, Seattle, WA.
- Kane, J. 2007. Zooplankton abundance trends on Georges Bank, 1977–2004. *ICES Journal of Marine Science*, 64: 909–919.
- Kotwicki, S., Horne, J. K., Punt, A. E., and Ianelli, J. N. 2015. Factors affecting the availability of walleye pollock to acoustic and bottom trawl survey gear. *ICES Journal of Marine Science*, 72: 1425–1439.
- Kubilius, R., Ona, E., and Calise, L. 2015. Measuring *in situ* krill tilt orientation by stereo photogrammetry: examples for *Euphausia superba* and *Meganyctiphanes norvegica*. *ICES Journal of Marine Science*, 72: 2494–2505.
- Ladd, C. 2007. Interannual variability of the Gulf of Alaska eddy field. *Geophysical Research Letters*, 34: 11605.
- Ladd, C., Cheng, W., and Salo, S. 2015. Gap winds and their effects on regional oceanography Part II: Kodiak Island, Alaska. *Deep Sea Research II*, doi: 10.1016/j.dsr2.2015.08.005.
- Ladd, C., Mordy, C. W., Kachel, N. B., and Stabeno, P. J. 2007. Northern Gulf of Alaska eddies and associated anomalies. *Deep Sea Research I*, 54: 487–509.
- MacLennan, D. N., Fernandes, P. G., and Dalen, J. 2002. A consistent approach to definitions and symbols in fisheries acoustics. *ICES Journal of Marine Science*, 59: 365–369.
- McBride, M. M., Dalpadado, P., Drinkwater, K. F., Godø, O. R., Hobday, A. J., Hollowed, A. B., Kristiansen, T., *et al.* 2014. Krill, climate, and contrasting future scenarios for Arctic and Antarctic fisheries. *ICES Journal of Marine Science*, 71: 1934–1955.
- McQuinn, I. H., Dion, M., and St Pierre, J. F. 2013. The acoustic multi-frequency classification of two sympatric euphausiid species (*Meganyctiphanes norvegica* and *Thysanoessa raschii*), with empirical and SDWBA model validation. *ICES Journal of Marine Science*, 70: 636–649.
- Method, R. D. 1986. Frame trawl for sampling pelagic juvenile fish. *CalCOFI Report*, 27: 267–278.
- Mueter, F. J., Bond, N. A., Ianelli, J. N., and Hollowed, A. B. 2011. Expected declines in recruitment of walleye pollock (*Theragra chalcogramma*) in the eastern Bering Sea under future climate change. *ICES Journal of Marine Science*, 68: 1284–1296.
- NOAA CCIEA. 2015. California Current Integrated Ecosystem Assessment (CCIEA) State of the California Current Report, 2015. A report of the CCIEA Team (NOAA Northwest, Southwest and Alaska Fisheries Science Centers) to the Pacific Fishery Management Council, 8 March 2015.
- Peterson, M. J., Mueter, F., Criddle, K., and Haynie, A. C. 2014. Killer whale depredation and associated costs to Alaskan sablefish, Pacific halibut and Greenland turbot longliners. *PLoS ONE*, 9: e88906.
- Petitgas, P. 1993. Geostatistics for fish stock assessments: a review and an acoustic application. *ICES Journal of Marine Science*, 50: 285–298.
- PFMC. 2013. Research and Data Needs. 2013. Pacific Fishery Management Council, Portland, OR.
- Pinchuk, A. I., Coyle, K. O., and Hopcroft, R. R. 2008. Climate-related variability in abundance and reproduction of euphausiids in the northern Gulf of Alaska in 1998–2003. *Progress in Oceanography*, 77: 203–216.
- Pinchuk, A. I., and Hopcroft, R. R. 2007. Seasonal variations in the growth rates of euphausiids (*Thysanoessa inermis*, *T. spinifera*, and *Euphausia pacifica*) from the northern Gulf of Alaska. *Marine Biology*, 151: 257–269.
- Reid, K., Croxall, J. P., Briggs, D. R., and Murphy, E. J. 2005. Antarctic ecosystem monitoring: quantifying the response of ecosystem indicators to variability in Antarctic krill. *ICES Journal of Marine Science*, 62: 366–373.
- Reiss, C. S., Cossio, A. M., Loeb, V., and Demer, D. A. 2008. Variations in the biomass of Antarctic krill (*Euphausia superba*) around the South Shetland Islands, 1996–2006. *ICES Journal of Marine Science*, 65: 497–508.
- Ressler, P. H., Dalpadado, P., Macaulay, G., and Skern-Mauritzen, M. 2015. Acoustic surveys of euphausiids and models of baleen whale distribution in the Barents Sea. *Marine Ecology Progress Series*, 527: 13–29.
- Ressler, P. H., De Robertis, A., and Kotwicki, S. 2014. The spatial distribution of euphausiids and walleye pollock in the eastern Bering Sea does not imply top-down control by predation. *Marine Ecology Progress Series*, 503: 111–222.
- Ressler, P. H., De Robertis, A., Warren, J. D., Smith, J. N., and Kotwicki, S. 2012. Developing an acoustic survey of euphausiid abundance to understand trophic interactions in the Bering Sea ecosystem. *Deep Sea Research II*, 65: 184–195.
- Richardson, A. J. 2008. In hot water: zooplankton and climate change. *ICES Journal of Marine Science*, 65: 279–295.
- Ricker, W. E. 1973. Linear regressions in fishery research. *Journal of the Fisheries Research Board of Canada*, 30: 409–434.
- Rivoirard, J., Simmonds, J., Foote, K. G., Fernandes, P., and Bez, N. 2000. Geostatistics for Estimating Fish Abundance. Blackwell Science, Oxford. 206 pp.
- Roopar, C. N., Zimmerman, M., Prescott, M. M., and Hermann, A. J. 2014. Predictive models of coral and sponge distribution, abundance and diversity in bottom trawl surveys of the Aleutian Islands, Alaska. *Marine Ecology Progress Series*, 503: 157–176.
- Sigler, M., Kuletz, K., Ressler, P. H., Friday, N., Wilson, C. D., and Zerbini, A. 2012. Marine predators and persistent prey in the south-east Bering Sea. *Deep Sea Research II*, 65: 292–303.
- Sigler, M., Napp, J. M., Stabeno, P. J., Heintz, R. A., Lomas, M. W., and Hunt, G. L., Jr. accepted for publication. Variation in annual production of copepods, euphausiids, and juvenile pollock in the southeastern Bering Sea. *Deep Sea Research II*.
- Simmonds, J., and MacLennan, D. 2005. Fishery Acoustic Theory and Practice. Blackwell Scientific Publications, London, UK.
- Smith, J. N., Ressler, P. H., and Warren, J. D. 2010. Material properties of Bering Sea euphausiids and other zooplankton. *Journal of the Acoustical Society of America*, 128: 2664–2680.
- Smith, J. N., Ressler, P. H., and Warren, J. D. 2013. A distorted wave Born approximation target strength model for Bering Sea euphausiids. *ICES Journal of Marine Science*, 70: 204–214.
- Stabeno, P. J., Bond, N. A., Hermann, A. J., Kachel, N. B., Mordy, C. W., and Overland, J. E. 2004. Meteorology and oceanography of the Northern Gulf of Alaska. *Continental Shelf Research*, 24: 859–897.
- Stabeno, P. J., Bond, N. A., Kachel, N. B., Salo, S. A., and Schumacher, J. D. 2001. On the temporal variability of the physical environment

- over the south-eastern Bering Sea. *Fisheries Oceanography*, 10: 81–98.
- Stauffer, G. 2004. NOAA Protocols for Groundfish Bottom Trawl Surveys of the Nation's Fishery Resources. US Department of Commerce, NOAA Technical Memorandum, NMFS-F/SPO-65. 205 pp.
- von Szalay, P. G., Wilkins, M. E., and Martin, M. M. 2009. Data report: 2007 Gulf of Alaska bottom trawl survey. NOAA Technical Memorandum, NMFS-AFSC-189. 247 pp.
- Williams, K., Rooper, C., and Towler, R. 2010a. Use of stereo camera systems for assessment of rockfish abundance in untrawlable areas and for recording pollock behavior during midwater trawls. *Fishery Bulletin US*, 108: 352–362.
- Williams, K., Towler, R., and Wilson, C. D. 2010b. Cam-Trawl: a combination trawl and stereo camera system. *Sea Technology*, 51: 45–51.
- Wilson, M. T. 2009. Ecology of small neritic fishers in the western Gulf of Alaska. I. Geographic distribution in relation to prey density and the physical environment. *Marine Ecology Progress Series*, 392: 223–237.
- Wilson, M. T., Jump, C. M., and Buchheister, A. 2009. Ecology of small neritic fishers in the western Gulf of Alaska. II. Consumption of krill in relation to krill standing stock and the physical environment. *Marine Ecology Progress Series*, 392: 239–251.
- Wilson, M. T., Mier, K. L., and Jump, C. M. 2013. Effect of region on the food-related benefits to age-0 walleye pollock (*Theragra chalcogramma*) in association with midwater habitat characteristics in the Gulf of Alaska. *ICES Journal of Marine Science*, 70: 1396–1407.
- Witteveen, B. H., De Robertis, A., Guo, L., and Wynne, K. M. 2015. Using dive behaviour and active acoustics to assess prey use and partitioning by fin and humpback whales near Kodiak Island, Alaska. *Marine Mammal Science*, 31: 255–278.
- Wood, S. N. 2006. *Generalized Additive Models: an Introduction with R*. Chapman and Hall, Boca Raton, FL.
- Wood, S. N., and Augustin, N. H. 2002. GAMs with integrated model selection using penalized regression splines and applications to environmental modelling. *Ecological Modelling*, 157: 157–177.
- Yang, M. S., Dodd, K., Hibpshman, R., and Whitehouse, A. 2006. Food habits of groundfishes in the Gulf of Alaska in 1999 and 2001 US. Department of Commerce, NOAA Technical Memorandum, NMFS-AFSC-164. 199 pp. <https://www.afsc.noaa.gov/Publications/AFSC-TM/NOAA-TM-AFSC-164.pdf>.
- Yang, M-S., and Nelson, M. W. 2000. Food habits of the commercially important groundfishes in the Gulf of Alaska in 1990, 1993, and 1996. US Department of Commerce, NOAA Technical Memorandum, NMFS-AFSC-112. 174 pp. <http://www.afsc.noaa.gov/refm/reem/doc/TechMemoAFSC112.pdf>.
- Zador, S. (Ed.) 2011. *Ecosystem Considerations for 2012, Stock Assessment and Fishery Evaluation Report*. North Pacific Fisheries Management Council, Anchorage, AK.
- Zador, S. 2014. *Ecosystem Considerations for 2014, Groundfish Stock Assessment and Fishery Evaluation Report*. 263 pp. <http://www.afsc.noaa.gov/REFM/Docs/2014/ecosystem.pdf>.

Handling editor: Stéphane Plourde